Determination of all relevant conduction electron scattering times in an exceptionally anisotropic arene conductor, the 12:7 pyrene hexafluoroantimonate radical cation salt

2003 J. Phys.: Condens. Matter 15 7085

(http://iopscience.iop.org/0953-8984/15/41/016)

INSTITUTE OF PHYSICS PUBLISHING JOURNAL OF PHYSICS: CONDENSED MATTER

J. Phys.: Condens. Matter **15** (2003) 7085–7093 PII: S0953-8984(03)67465-5

Determination of all relevant conduction electron scattering times in an exceptionally anisotropic arene conductor, the 12:7 pyrene hexafluoroantimonate radical cation salt

A Kaiser, T Wokrina, B Pongs and E Dormann

Physikalisches Institut, Universität Karlsruhe (TH), D-76128 Karlsruhe, Germany

Received 11 August 2003
Published 3 October 2003
Online at stacks.iop.org/JPhysCM/15/7085

Abstract

For $(pyrene)_{12}(SbF_6)_7$ a 10^4:1 anisotropy of the microwave conductivity is observed. We show that the timescale for the end of the one-dimensional motion of the conduction electron spins derived by analysis of the frequency and temperature dependence of the proton spin–lattice relaxation and of the electron spin resonance linewidth and relaxation times is governed to a comparable degree by perpendicular-to-stack hopping and by interaction with intrastack paramagnetic localized defects in these crystals. The electron spin self-diffusion coefficient derived for the magnetic field gradient parallel to the pyrene stacking direction is therefore influenced by perpendicular-to-stack motion as well.

1. Introduction

Quasi-one-dimensional conductors received their name due to the very large anisotropy of their electrical conductivity, exceeding $\sigma_\parallel/\sigma_\perp = 10^4$:1 in favourable cases. Since they are regular three-dimensional solids, their transverse electron mobility is non-zero, however, which is the reason for the 'quasi' in the name. The exact degree of anisotropy is difficult to obtain from conductivity measurements, however, because a slight misorientation, occasionally inevitable due to the mosaic-like structure of the real single crystal, may give rise to the inadvertent measurement of a small component of the parallel-to-stack mobility that is misinterpreted as a finite perpendicular mobility value. Thus, it is very desirable to combine different independent techniques for testing the anisotropy of the conduction electron spin and the charge motion in a nominally quasi-one-dimensional conductor.

In this investigation we combine microwave electrical conductivity data $(\sigma_\parallel(T), \sigma_\perp(T))$ with measurement of the anisotropy of the conduction electron spin diffusion constant $(D(\theta))$ that is derived by analysis of the electron spin echo decay in a static applied magnetic

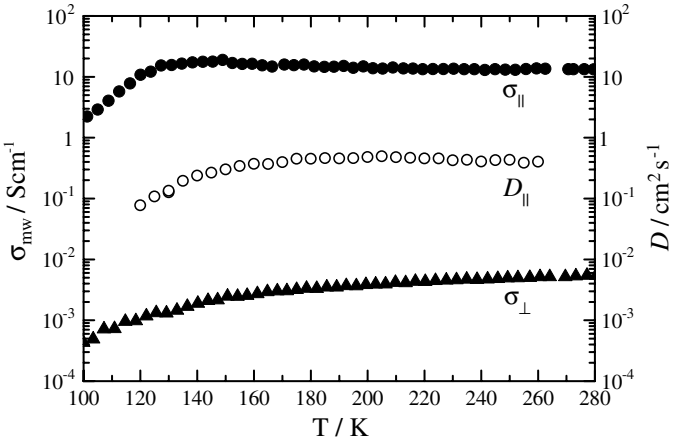

Figure 1. The temperature dependence of the microwave (10 GHz) conductivity σ parallel or perpendicular [6], and of the spin diffusion constant D ($\nu_e = 425$ MHz) parallel to the PY stacking direction in the 12:7 PY hexafluoroantimonate salt.

field gradient, SGESE, in analogy to the nuclear spin self-diffusion coefficient known from nuclear magnetic resonance (NMR) in liquids [1, 2]. Furthermore, we analyse the frequency dependence of the nuclear spin–lattice relaxation that reflects the time constant τ^* describing the termination of the one-dimensional diffusive conduction electron spin dynamics [3, 2]. τ^* can be influenced by the interaction of the conduction electron with intrastack paramagnetic defects (τ_{ce-d}) as well as by the perpendicular-to-stack hopping motion of the conduction electron, $\tau_\perp$. Therefore, τ_{ce-d} is derived below from an earlier quantitative analysis of the temperature, frequency, and orientation dependence of the electron spin resonance (ESR) linewidth and relaxation rate [4]. $\tau_\perp$ can be estimated from microwave conductivity $\sigma_\perp$ and diffusion coefficient $D_\perp$, but is also accessible from a combination of τ^* and τ_{ce-d}. Finally, we take the information about the restriction of quasi-one-dimensional diffusive conduction electron spin motion that can be extracted from the SGESE decay for very long observation time, in the several microsecond time window, into account. Thus we aim at an especially complete picture of the conduction electron spin and charge dynamics of a quasi-one-dimensional organic conductor.

We use an organic conductor built up from pyrene (PY) radical cations as a model system for this experimental attempt [5]. Earlier ESR analysis gave a proof that the 12:7 radical cation salt with hexafluoroantimonate anions, i.e. $(PY)_{12}(SbF_6)_7$, has a sufficiently simple crystal structure with one-dimensional stacks of parallel oriented PY molecules [4]. In spite of a relatively high concentration of localized Curie-like paramagnetic defects of about $(2–3) \times 10^{-2}$ per formula unit $(PY)_{12}(SbF_6)_7$, these radical cation salts show a well-defined Peierls transition to a low temperature non-metallic phase at about $T_P = 116 \pm 2$ K [4, 6]. Most promisingly, these quasi-one-dimensional conductors exhibited not only a 10^4:1 anisotropy of their microwave electrical conductivity, but also a clear distinction between the relative temperature dependences of $\sigma_\parallel(T)$ and $\sigma_\perp(T)$ (see figure 1) [4, 6]. Whereas $\sigma_\perp(T)$ increases with temperature as expected for thermally activated hopping motion, $\sigma_\parallel(T)$ decreases in a metal-like fashion with increasing $T > 145$ K. Thus, $(PY)_{12}(SbF_6)_7$ crystals present one of the rare examples of a radical cation salt built up from pure aromatic hydrocarbon molecules, where $\sigma_\perp(T)$ cannot simply be described as a small portion of $\sigma_\parallel$, causing $\sigma_\perp(T)$ and the observed microwave conductivity anisotropy to be more reliable than usual.

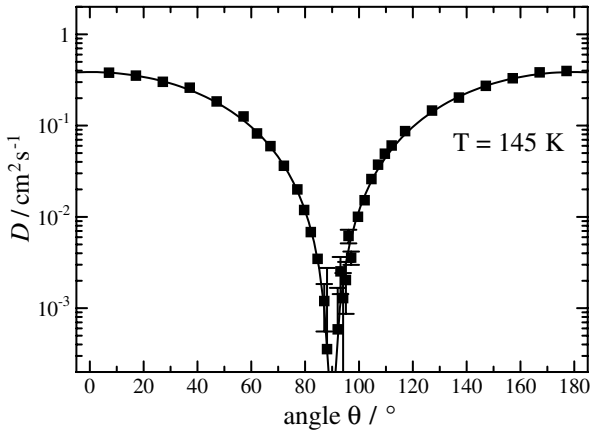

Figure 2. Variation of the spin diffusion constant D with the orientation of the magnetic field gradient with respect to the PY stacking axis in the 12:7 PY hexafluoroantimonate salt ($T = 145$ K, $\nu_e = 425$ MHz; fit values $D_\parallel = 0.386$ cm^2 s^{-1}, $D_\perp \leqslant 3.3 \times 10^{-5}$ cm^2 s^{-1}).

After giving a short collection of the relevant experimental references and results in section 2, we present the models used for data analysis, aiming at obtaining the anisotropy of the electron spin diffusion, in section 3.1. Via the hyperfine interaction, the PY protons can be used to monitor the conduction electron spin dynamics. The analysis of the frequency dependence of the proton spin–lattice relaxation yields the quantity τ^*, indicating the end of the purely one-dimensional conduction electron spin dynamics (3.2). In section 4, we discuss the values (and the interpretation) of the various time constants characterizing the limits of one-dimensional electron spin dynamics thus obtained for $(PY)_{12}(SbF_6)_7$ and compare them with the time constants derived for the exchange interaction of the conduction electrons with localized paramagnetic defects. Concluding remarks follow in section 5.

2. Experimental details and results

The electrochemical growth of plate-like single crystals of $(PY)_{12}(SbF_6)_7$ has been described earlier [4, 5]. The electron spin (self-) diffusion constant $D(\theta)$ was derived at $\nu_e = 425$ MHz and 9.5 GHz by analysis of the electron spin echo decay in a static magnetic field gradient for varied orientation θ of the PY stacking direction with respect to the gradient direction and for varied temperature (see figures 1 and 2 for examples). For description of the experimental details we refer the reader to [7, 8]. The proton–nuclear spin–lattice relaxation rate $T_{1,p}^{-1}$ was derived as a function of temperature for proton Larmor frequencies $\nu_p = 300$ and 53 MHz by the inversion–recovery technique and at $\nu_p = 14$ MHz with the help of the Overhauser shift method [9, 10] (figure 3). In order to probe lower Larmor frequencies, relaxation was also analysed in the rotating frame, $T_{1\rho}$ [9, 11] (see the inset to figure 3).

3. Data analysis

3.1. Electron spin diffusion

The anisotropy of the electron spin diffusion constant $D(\theta)$ can be reasonably well reproduced by [2, 7]

$$D(\theta) = D_\parallel \cos^2\theta + D_\perp \sin^2\theta. \tag{1}$$

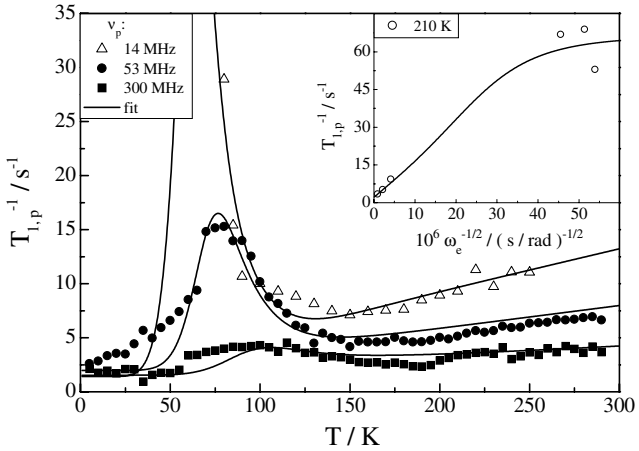

Figure 3. The temperature dependence of the proton spin–lattice relaxation rate for three Larmor frequencies (ν_p = 14, 53, and 300 MHz) versus temperature, or for fixed temperature T = 210 K, versus the square root of the inverse Larmor frequency ω_e (inset), derived for a 12:7 PY hexafluoroantimonate salt sample. For the parameters of the fit see table 1.

This is visualized in figure 2, with $D(\theta)$ data derived in the radio-frequency range, ν_e = 425 MHz. The fit yields $D_\parallel = 0.386\,\mathrm{cm^2\ s^{-1}}$ and an upper limit of $D_\perp \leqslant 3.3\times10^{-5}\,\mathrm{cm^2\ s^{-1}}$, indicating an anisotropy $D_\parallel/D_\perp \geqslant 10^4$ at T = 145 K. The temperature dependence of $D_\parallel(T)$ for the same crystal, derived at the same frequency, is compared with that of the microwave electrical conductivity (10.2/10.3 GHz [6]) in figure 1.

A larger dynamical range can be exploited at ν_e = 9.5 GHz for the echo decay in the static magnetic field gradient. Thus, in addition to $D_\parallel$ (290 K) = 0.60 cm^2 s^{-1} and $D_\perp$ (290 K) $\leqslant 2\times10^{-4}$ cm^2 s^{-1} derived for another $(PY)_{12}(SbF_6)_7$ single crystal, the Neuman model [12] describing the influence of restrictions (chain length l) on free diffusion has been fitted to the data [7]. This model predicts l-dependent spin echo decay with pulse separation τ:

$$\frac{A(l,2\tau)}{A(l,0)} = \exp\left\{-\frac{2\tau}{T_2} - \frac{8\gamma_e^2G^2l^4}{D\pi^6}\sum_{n=0}^{\infty}\frac{1}{(2n+1)^6}\left[2\tau - \frac{3-4\mathrm{e}^{-Q\tau}+\mathrm{e}^{-2Q\tau}}{Q}\right]\right\} \tag{2}$$

with

$$Q = D\frac{(2n+1)^2\pi^2}{l^2} \tag{3}$$

for magnetic field gradient G. The SGESE decay is then calculated by folding equation (2) with the weight factor $P(l)$ of the chain length distribution:

$$\frac{M(2\tau)}{M(0)} = \frac{A(l,2\tau)}{A(l,0)} \otimes P(l). \tag{4}$$

Assuming an exponentially decreasing distribution function of chain lengths l, i.e.

$$P(l) = (l/\bar{l}^2)\exp(-l/\bar{l}), \tag{5}$$

a characteristic (average) length $\bar{l}$ = 23 μm was derived for $(PY)_{12}(SbF_6)_7$ at 290 K. This length $\bar{l}$ is smaller by a factor of about 4 compared to those for other radical cation salts built up from fluoranthene [13] or perylene [14]. A similar value, i.e. $\bar{l}$ = 17 μm, was observed for a proton-irradiation-damaged fluoranthene radical cation salt crystal with 10^{-2} defects per formula unit [7]. The small $\bar{l}$ value might thus be related to the large content of paramagnetic

defects in $(PY)_{12}(SbF_6)_7$ crystals, identified by static magnetic susceptibility measurements. It amounts to about (2–3) $\times 10^{-2}$ defects per formula unit for as grown crystals [4], up to an order of magnitude higher than in many other arene salts [15].

3.2. Proton spin–lattice relaxation

The analysis of the temperature and frequency dependence of the nuclear spin–lattice relaxation is an established method for the monitoring of molecular reorientation [16–18] and electron spin dynamics [3, 16, 17, 19, 20] in radical cation salts of arenes with complex anions. We refer the reader to these references for the relations describing the influence of SbF_6 reorientations on ^{19}F nuclear spin relaxation. For protons, the influence of ^{19}F–^1H magnetic dipolar interaction, modulated by SbF_6 reorientation jumps, and of ^1H–^1H interaction, modulated by PY librational and vibrational motion, on the spin–lattice relaxation rate can be parametrized as [16, 17, 21]

$$(T_{1,p})^{-1}_{BPP} = K_{HF}(J(\tau_{HF}, (\omega_H - \omega_F)) + 3J(\tau_{HF}, \omega_H) + 6J(\tau_{HF}, (\omega_H + \omega_F))) + K_{HH}(J(\tau_{HH}, \omega_H) + 4J(\tau_{HH}, 2\omega_H)) \tag{6}$$

with

$$J = \frac{\tau_i}{1 + (\omega\tau_i)^2} \tag{7}$$

and a simple Arrhenius law for τ_i:

$$\tau_i = \tau_{\infty,i} \exp(\Delta E_i / k_B T). \tag{8}$$

For distinction from the Korringa-like conduction electron contribution to the proton spin–lattice relaxation, $(T_{1,p})^{-1}_K$, we use $(T_{1,p})^{-1}_{BPP}$ for the molecular-motion-induced proton relaxation contribution, with

$$(1/T_{1,p})^{-1} = (1/T_{1,p})^{-1}_K + (1/T_{1,p})^{-1}_{BPP}. \tag{9}$$

The latter contribution is responsible for the low temperature BPP-like maxima [21] in figure 3.

For the conduction electron (modified Korringa) contribution to the proton spin–lattice relaxation, a decomposition into frequency dependent and independent parts [3, 17, 19, 20]:

$$(T_{1,p}T)^{-1}_K = C_1\left(\chi_{ce}, \frac{\tau^*}{\tau_\parallel}\right)\left[\frac{1 + [1 + (\omega_e\tau^*)^2]^{1/2}}{2[1 + (\omega_e\tau^*)^2]}\right]^{1/2} + C_2(\chi_{ce}) \tag{10}$$

is generally used, corresponding to long wavelength ($q \approx 0$) and short wavelength ($q = 2k_F$) excitations.

The relevant parameters are compiled in table 1. The influence of the molecular motions predominates in the low temperature range. The activation energies ΔE_{HF} and ΔE_{HH} in the 20–60 meV range are typical for anion and arene motions [17, 18]. Like in fluoranthene [16] and perylene [17] radical cation salts, we observe that the slowing down of the counterion reorientation rate into the 300–14 MHz range (giving rise to the BPP maxima) occurs roughly at the actual Peierls transition temperature (i.e. $T_P = 116$ K for $(PY)_{12}(SbF_6)_7$). The conduction electron contribution predominates at temperatures above 150 K. The $T_{1\rho}$ data for the low ω_e range (see the inset to figure 3) are indispensable for a reasonably accurate estimate of the time constant τ^* [11], describing the ending of the purely one-dimensional diffusive conduction electron spin dynamics caused by the relaxing influence of an intrastack defect (τ_{ce-d}) and/or the escape of the electron from its own stack to a neighbouring stack by hopping motion ($\tau_\perp$). C_2 is negligibly small compared to C_1 (table 1), which is enhanced by the huge factor $(\tau^*/\tau_\parallel)^{1/2} \approx 580$ in $(PY)_{12}(SbF_6)_7$.

Table 1. Fit parameters for proton (and ^{19}F) spin–lattice relaxation contributions in $(\text{pyrene})_{12}(SbF_6)_7$ derived from a fit to figure 3 (updated ^{19}F data compared to [18]). For definitions of the parameters, see [17, 18] and the text.

	^{1}H		^{19}F	
K_{HF}	5.18×10^7 s^{-2}	K_{FH}	1.48×10^8 s^{-2}	
$\tau_{\infty,HF}$	1.74×10^{-9} s	$\tau_{\infty,FH}$	1.74×10^{-9} s	
ΔE_{HF}	21.6 meV	ΔE_{FH}	21.6 meV	
			$i = 1$	$i = 2$
K_{HH}	3.08×10^9 s^{-2}	K_{FFi}	9.83×10^8 s^{-2}	$1.1/1.3 \times 10^9$ s^{-2}
$\tau_{\infty,HH}$	2.68×10^{-12} s	$\tau_{\infty,FFi}$	3.76×10^{-12} s	$19.7/0.37 \times 10^{-17}$ s
ΔE_{HH}	43.2 meV	ΔE_{FFi}	59.4 meV	382/213 meV
C_1T(210 K)	64.4 s^{-1}			
C_2T(210 K)	Negligible			
τ^*(210 K)	1.095 ns			

4. Discussion

It is well established that the scattering time $\tau_\parallel$ of the conduction electrons in quasi-one-dimensional organic conductors is rather short in their high temperature metallic phase between room temperature and the Peierls transition temperature [22]. The reported values of $\tau_\parallel$ in the several femtosecond range correspond to mean free path values not much larger than some intermolecular distances along the stack. These $\tau_\parallel$ values seemed to fit to the observed self-diffusion coefficients of the electron spins ($D_\parallel$) in the 1–4 cm^2 s^{-1} range in cases where the Fermi velocity (v_F) was known and the validity of the relation $D_\parallel = v_F^2\tau_\parallel$ could be checked quantitatively [14].

The situation is more complicated in $(PY)_{12}(SbF_6)_7$. At microwave frequency, the conductivity $\sigma_\parallel = 10$–20 S cm^{-1} is already much smaller than the optical conductivity of 1.6×10^3 S cm^{-1} [22] (figure 1). Furthermore, the observed values of the diffusion constant $D_\parallel = (0.4$–$0.6)$ cm^2 s^{-1} (derived with SGESE experiments using microsecond pulse separations) are clearly lower than the estimate $D_\parallel \approx 3$ cm^2 s^{-1} calculated from $\tau_\parallel = 3.3$ fs [22] and the Fermi velocity $v_F = (2.9$–$3.1) \times 10^5$ m s^{-1} estimated from the Pauli paramagnetic susceptibility or band filling (with $m^* \approx m_e$). Thus the experimentally determined value of $D_\parallel$ seems to be reduced by the intrastack defects forcing the electron to leave its 'own' stack in order to pass by. This passing by is indeed possible for measurements probing conduction electron motion on the microsecond timescale, as shown below.

An estimate of the transverse hopping time constant $\tau_\perp \geqslant 0.19$–$0.57$ ns can be obtained from the upper limit of $D_\perp$, i.e. $D_\perp \leqslant 3.3 \times 10^{-5}$ cm^2 s^{-1}, and the relation $D_\perp = d_\perp^2/\tau_\perp$ (varying $d_\perp$ from 0.8 to 1.37 nm, i.e., from intra-unit-cell to cell-to-cell jumps). At least this lower limit of the timescale $\tau_\perp$ (table 2) allows for thousands of perpendicular-to-stack jumps within the timescale used for the SGESE spin diffusion measurements. On the other hand, even this lower limit of $\tau_\perp$ already indicates a five orders of magnitude anisotropy of the scattering times $\tau_\parallel$ versus $\tau_\perp$. Another lower limit for the transverse hopping time constant $\tau_\perp$ is obtained from the experimental values of the (supposedly) transverse conductivity (figure 1). The interpretation as hopping conductivity, $\sigma_\perp = \frac{\partial n_h}{\partial E} e^2 d_\perp^2/\tau_\perp$, gives $\tau_\perp$ in the 1–2 ns range (table 2).

Especially clear-cut information on the timescale of the termination of the purely one-dimensional diffusive motion of the conduction electron spins is deduced from the ω_e

Table 2. Time constants characterizing the limits of one-dimensional electron spin dynamics in the 12:7 PY hexafluoroantimonate salt, together with references and respective defining relations.

Time constant	Value	Relation
$\tau_{\parallel}$(300 K)	3.3 fs	[22]
$\tau_{\perp}$(145 K)	$\geqslant$0.19–0.57 ns	$D_{\perp} = d_{\perp}^2/\tau_{\perp}$
$\tau_{\perp}$(210 K)	$\geqslant$0.8–2.5 ns	$\sigma_{\perp}$ (hopping)
τ^*(210 K)	1.095 ns	$T_{1,\mathrm{p}}(\nu_{\mathrm{e}})$
$\tau_{\mathrm{d-ce}}$(250 K)	0.261 ns	$1/T_{2,\mathrm{e}}(\theta, \nu_{\mathrm{e}})$ [4]
$\tau_{\mathrm{ce-d}}$(250 K)	3.24 ns	$\tau_{\mathrm{ce-d}} = (\chi_{\mathrm{ce}}/\chi_{\mathrm{d}})\tau_{\mathrm{d-ce}}$
$\tau_{\mathrm{ce-d}}$(210 K)	1.85 ns	$\tau_{\mathrm{ce-d}} = (\chi_{\mathrm{ce}}/\chi_{\mathrm{d}})\tau_{\mathrm{d-ce}}$
$\tau_{\perp}$(210 K)	2.68 ns	$(\tau^*)^{-1} = (\tau_{\mathrm{ce-d}})^{-1} + (\tau_{\perp})^{-1}$
$t_{\parallel,\max}$(290 K)	4.4 μs	$\bar{l}_{\parallel} = (2D_{\parallel}t_{\parallel,\max})^{1/2}$

dependence of the proton 'Korringa-like' relaxation; see equation (10) and figure 3. $\tau^* = 1.1$ ns is obtained at $T = 210$ K. The quantity τ^* can be—and actually is—shorter than $\tau_{\perp}$. This happens if the electron spin relaxes at an intrastack impurity after the time interval $\tau_{\mathrm{ce-d}}$ without hopping to the neighbouring stack. The ratio $\tau^*{:}\tau_{\parallel} \approx 3 \times 10^5$ (table 2) again proves definitely the 'one-dimensional' character of $(\mathrm{PY})_{12}(\mathrm{SbF_6})_7$.

Further information on the role of the paramagnetic defects in $(\mathrm{PY})_{12}(\mathrm{SbF_6})_7$ for τ^* is obtained from ESR [4]. The defects and conduction electrons interact by classical magnetic dipolar interaction and by exchange interaction. Due to the extremely weak spin–orbit coupling in one-dimensional metals that are built up from pure hydrocarbon molecules, a bottleneck situation of the spin–lattice relaxation is found in $(\mathrm{PY})_{12}(\mathrm{SbF_6})_7$. Zeeman energy is transferred between defects (d) and conduction electrons (ce), back and forth, before the relaxation to the lattice/bath. Thus a detailed balance relation is obeyed, i.e. $\tau_{\mathrm{ce-d}} = (\chi_{\mathrm{ce}}/\chi_{\mathrm{d}})\tau_{\mathrm{d-ce}}$. From the frequency dependence of electron spin $T_2(\theta, \nu_{\mathrm{e}})$, the absolute value $\tau_{\mathrm{d-ce}}(250\ \mathrm{K}) = 0.261$ ns was derived for $(\mathrm{PY})_{12}(\mathrm{SbF_6})_7$ [4]. Using $\chi_{\mathrm{ce}}(T)$, $\chi_{\mathrm{d}}(T)$, and $\tau_{\mathrm{d-ce}}(T)$ of [4] the time constant characterizing the relaxation from the conduction electron to the localized defect, $\tau_{\mathrm{ce-d}}$, is derived (table 2). There is no question that the sum of the two processes, i.e. the relaxation to the impurity spins, $(\tau_{\mathrm{ce-d}})^{-1}$, plus the jumping to the neighbouring stack, with the rate $(\tau_{\perp})^{-1}$, determine the end of the one-dimensional conduction electron spin dynamics (table 2). This superposition of $(\tau_{\perp})^{-1} = R_{\perp}\exp(-\Delta E/k_{\mathrm{B}}T)$ (with $\Delta E = 0.029$ eV, derived from microwave conductivity $\sigma_{\perp}(T)$) and $(\tau_{\mathrm{ce-d}})^{-1}$, derived from ESR analysis [4], was used for $\tau^*(T)$ of equation (10) in the fit in figure 3.

The strictly one-dimensional motion of the conduction electron spins is thus restricted by the distribution of localized defects encountered on the stack in $(\mathrm{PY})_{12}(\mathrm{SbF_6})_7$. The possibility of applying a whole 'zoo' of resonance methods to the quasi-one-dimensionally conducting arene radical cation salts gives access to experimental evidence that the conduction electron spin must be able to pass by a localized intrastack defect by perpendicular motion. From the detailed analysis of the electron spin echo decay in a static magnetic field gradient parallel to the stacking axis, the characteristic length $\bar{l}_{\parallel} = 23$ μm of the restricted diffusion was derived for $(\mathrm{PY})_{12}(\mathrm{SbF_6})_7$ at 290 K (section 3.1 and [7]). The straightforward interpretation of this finding is that only at $l_{\parallel}$ does the electron hit an obstacle that is of such geometrical extent that it cannot be passed by perpendicular jumps within the microsecond timescale of the ESR spin echo experiment. Since $t_{\parallel,\max}$ (table 2) is about three orders of magnitude larger than τ^* or $\tau_{\mathrm{ce-d}}$, and $\bar{l}_{\parallel} = 23$ μm is a factor of 66 larger than the parallel diffusion length within $\tau^* \approx 1$ ns, the electron spin must be able to continue its motion along the preferred direction even after an encounter with a localized defect.

Finally, we want to discuss the qualitative T dependence of $\sigma_\parallel(T)$, $\sigma_\perp(T)$, and $D_\parallel(T)$. The microscopic relations $D_\parallel = v_F^2\tau_\parallel$ and $\sigma_\parallel = n(T)(e^2/m^*)\tau_\parallel$ would suggest that $\sigma_\parallel(T)$ decreases more quickly with T than $D_\parallel(T)$ on approach to the Peierls transition temperature $T_P = 116$ K due to the decrease of $n(T)$ indicated by the decrease of $\chi_{ce}(T)$ [6]. This is not shown by the data presented in figure 1. Instead, the similarity of $D_\parallel(T)$ and $\sigma_\perp(T)$ is striking. We must thus assume that the reduction of $D_\parallel$ by a factor of 5 compared to the estimated value $v_F^2\tau_\parallel$ is caused by the necessity of perpendicular motion in order to pass local defects, and that this composed motion introduces the activation law temperature dependence of $\sigma_\perp(T)$ also into the T dependence of the reduced effective values of $D_\parallel(T)$.

5. Conclusions

We presented the first example of a quasi-one-dimensional conductor built up by stacked arene radical cations where all relevant conduction electron scattering times could be derived experimentally. Indeed, the 12:7 PY hexafluoroantimonate radical cation salt is a rather special quasi-one-dimensional organic conductor. It is one of the rare examples where the experimental results of the measurement of $\sigma_\perp(T)$, the microwave conductivity perpendicular to the stacking direction of the aromatic hydrocarbon molecules, is not simply a small component of $\sigma_\parallel(T)$, but shows clearly a different—i.e. activated—temperature dependence, in addition to a large anisotropy of $\sigma_\parallel{:}\sigma_\perp \approx 10^4{:}1$. This is in part due to the fact that plate-like single crystals of $(PY)_{12}(SbF_6)_7$ could be grown. Typically, deviation from the standard needle-like shape of quasi-one-dimensional conductors is obtained for crystals with a comparably large concentration of defects. This is the case for $(PY)_{12}(SbF_6)_7$, too, where a concentration of (2–3) $\times 10^{-2}$ Curie paramagnetic localized defects per formula unit has been determined, making, e.g., a more detailed x-ray structural analysis impossible (except as regards unit-cell parameters and space groups [4, 5]). The seemingly large defect concentration should not be overstressed, however. First of all, it does not prevent the $10^4{:}1$ ratio of $\sigma_\parallel/\sigma_\perp$; second, it allowed the detailed and unique analysis reported above; and, finally, the given concentrations have to be looked at from the correct point of view: (2–3) $\times 10^{-2}$ Curie paramagnetic defects per formula unit means one defect per 400–600 PY molecules or only (5–8) $\times 10^{-5}$ Curie defects per atom, if expressed in terms familiar for inorganic compounds! Furthermore, most of the defects tend to be accumulated at the surfaces of radical cation salts [8, 19]. Nevertheless, defects within the stack of quasi-one-dimensional organic conductors break the one-dimensional conducting path; they thus force the conduction electron spin to interact with this defect and to leave its own stack in order to pass the local obstacle, reducing the absolute value of the effective parallel-to-stack mobility. All these phenomena have been demonstrated above for $(PY)_{12}(SbF_6)_7$, where the rate constant $(\tau^*)^{-1}$ for the end of one-dimensional spin dynamics, $(\tau^*)^{-1} = (\tau_{ce-d})^{-1} + (\tau_\perp)^{-1}$, could be separated into its different contributions. The value of τ^* was derived via NMR. The diffusive decay of long wavelength conduction electron spin density wave excitations gives rise to a typical $\omega_e^{-1/2}$ increase of the nuclear spin–lattice relaxation rate for decreasing nuclear spin Larmor frequency ($\omega_p = (\gamma_p/\gamma_e)\omega_e$) [3]. The rate $(\tau^*)^{-1}$, influenced in $(PY)_{12}(SbF_6)_7$ by the intrastack paramagnetic defects, sets an end to the diffusive decay and to the frequency dependence of the proton spin–lattice relaxation, $T_{1,p}$. On the other hand, τ_{ce-d} is obtained from ESR and is evidently linked to the defects. The exchange modulation of the mutual dipolar interaction of localized defect spins and conduction electron spins in the bottleneck system balances the defect-to-conduction electron and the conduction electron-to-defect relaxations, τ_{d-ce} and τ_{ce-d}, respectively. Thus, the values of $(\tau_{ce-d})^{-1}$ can be deduced from the known dependences of the ESR T_1, T_2, and linewidth on temperature,

crystal orientation, and electron spin Larmor frequency. For $(PY)_{12}(SbF_6)_7$, table 2 indicates that τ^* and τ_{ce-d} have the same order of magnitude, but are not identical.

We have shown that a consistent value and temperature dependence of $\tau_\perp$, the time constant for the perpendicular hopping of the conduction electrons, can be given for $(PY)_{12}(SbF_6)_7$ by analysis of the microwave perpendicular-to-stack conductivity $\sigma_\perp(T)$ and by the decomposition of $(\tau^*(T))^{-1}$ into the two contributions $(\tau_{ce-d})^{-1}$ and $(\tau_\perp)^{-1}$. The value of $\tau_\perp$ is of the same order of magnitude as τ^* and τ_{ce-d}. In addition, the proof of an extended path—or, better, passing—of the conduction electron spins in the direction of the PY stacks ($\bar{l}_\parallel = 23\ \mu$m for pulsed ESR sensitive to the microsecond range) has been given experimentally. For a crystal with a comparably high content of intrastack defects and short time interval τ_{ce-d}, this long distance travel $l_\parallel$ unequivocally requires also a perpendicular-to-stack hopping motion. Thus we conclude that 'slow' experiments (compared to optical reflectivity) deliver only effective values for $\sigma_\parallel(T)$ and $D_\parallel(T)$, that are influenced noticeably by the perpendicular motion in $(PY)_{12}(SbF_6)_7$. It is an obvious challenge for future research to derive absolute experimental values, and not only upper limits, for the conduction electron motion perpendicular to the preferred direction also in quasi-one-dimensional organic conductors of lower defect content and possibly even higher degree of anisotropy than reported here for the 12:7 PY hexafluoroantimonate salt.

Acknowledgments

We thank I Odenwald for crystal growth and A Feintuch and N Kaplan for discussions. This work was financially supported by the Deutsche Forschungsgemeinschaft within the Sonderforschungsbereich 195 (Universität Karlsruhe (TH)) and project Do 181/10.

References

[1] Torrey H C 1956 *Phys. Rev.* **104** 563
[2] Mehring M 1987 *Low-Dimensional Conductors and Superconductors* ed D Jérome and L G Caron (New York: Plenum) p 185
[3] Soda G, Jérome D, Weger M, Alizon J, Gallice J, Robert H, Fabre J M and Giral L 1977 *J. Physique Coll.* **38** 931
[4] Pongs B and Dormann E 2002 *Phys. Rev.* B **65** 144451
[5] Enkelmann V 1988 *Adv. Chem. Ser.* **217** 177
[6] Pongs B, Matejcek S, Kelemen M T, Buschhaus C and Dormann E 2001 *Synth. Met.* **120** 839
[7] Wokrina T 2002 Räumlich eingeschränkte Elektronen-Spindiffusion in quasi-eindimensionalen organischen Leitern *PhD Thesis* (Aachen: Shaker)
[8] Wokrina T, Gmeiner J, Kaplan N and Dormann E 2003 *Phys. Rev.* B **67** 054103
[9] Abragam A 1989 *Principles of Nuclear Magnetism* (Oxford: Clarendon)
[10] Denninger G, Dormann E and Schwoerer M 1987 *Synth. Met.* **19** 355
[11] Kaiser A, Pongs B and Dormann E 2003 *Synth. Met.* **135/136** 547
[12] Neuman C H 1974 *J. Chem. Phys.* **60** 4508
[13] Ruf R, Kaplan N and Dormann E 1995 *Phys. Rev. Lett.* **74** 2122
Ruf R, Kaplan N and Dormann E 1995 *Phys. Rev. Lett.* **75** 1237
[14] Wokrina T, Dormann E and Kaplan N 1996 *Phys. Rev.* B **54** 10492
[15] Pongs B, Fischer G and Dormann E 2002 *J. Phys.: Condens. Matter* **14** 8655
[16] Höptner W, Mehring M, von Schütz J U, Wolf H C, Morra B S, Enkelmann V and Wegner G 1982 *Chem. Phys.* **73** 253
[17] Nemec G, Illich V and Dormann E 1998 *Synth. Met.* **95** 149
[18] Kaiser A, Pongs B, Fischer G and Dormann E 2001 *Phys. Lett.* A **282** 125
[19] Sachs G and Dormann E 1988 *Synth. Met.* **25** 157
[20] Jérome D and Schulz H J 1982 *Adv. Phys.* **31** 299
[21] Bloembergen N, Purcell E M and Pound R V 1948 *Phys. Rev.* **73** 679
[22] Geserich H P, Koch B, Ruppel W, Wilckens R, Schweitzer D, Enkelmann V, Wegner G, Wieners G and Keller H J 1983 *J. Physique Coll.* **44** C3 1461